Available online at www.sciencedirect.com
ScienceDirect
Journal of Photochemistry and Photobiology A: Chemistry 192 (2007) 98–104
Journal of Photochemistry and Photobiology A:Chemistry
www.elsevier.com/locate/jphotochem

Photoinitiation of acrylamide polymerization by Fe_2O_3 nanoparticles

Alexander L. Stroyuk *, Ivan V. Sobran, Stephan Ya. Kuchmiy

Pysarzhevski Institute of Physical Chemistry of Nat. Acad. Sci. of Ukraine, 31, Nauky av., 03028 Kyiv-028, Ukraine

Received 5 February 2007; received in revised form 10 April 2007; accepted 10 May 2007
Available online 16 May 2007

Abstract

Photocatalytic activity of α-Fe_2O_3 nanoparticles in the acrylamide photopolymerization in aqueous solutions has been investigated. The photoreaction proceeds efficiently both in degassed and air-exposed solutions, at low photoinitiator concentrations ($[Fe_2O_3] < 1 \times 10^{-3}$ M), under the near UV and the visible light ($\lambda < 600$ nm), and results in the formation of polyacrylamide with relatively high molecular mass (1.2×10^6 g/mole in degassed solutions and 0.7×10^6 g/mole in air-exposed solutions).

Kinetics of the photoinduced acrylamide polymerization has been studied and optimal reaction conditions determined. It has been shown that the quantum yields of the photopolymerization and the photoinitiation in the systems under investigation do not exceed, respectively, 10^2 and 10^{-2}.

The mechanism of the photopolymerization has been proposed, which includes the photoinitiation stage with the participation of acrylamide radicals, the latters originating from the monomer oxidation by the photogenerated Fe_2O_3 valence band holes, the free-radical chain growth and subsequent recombination of the growing macroradicals.

Keywords: Semiconductor nanoparticles; Photocatalysis; Fe_2O_3; Photopolymerization; Acrylamide; Polyacrylamide

1. Introduction

Photoinduced polymerization of unsaturated compounds is of great importance not only for the production of polymer materials but also for the implementation of a number of advanced technologies. The latters are the optical information recording, the production of polygraphic forms, printed-circuit plates for the microelectronics, miniature surgical instruments, lenses and prostheses with complex topology and micron (submicron) resolution, the removable polymeric templates for lithography and stereolithography, etc. [1–6]. Successful implementation of some of these technologies sometimes demands a specific combination of the properties of monomers and polymeric products as well as polymerization conditions. For example, photocurable compositions for the digital stereolithography are required to be sensitive to the visible light illumination of a computer-guided projecting system and produce upon the illumination an easily removable water-soluble polymeric template. The latter requirement can be met by the utilization of monomers, converting upon the illumination into water-soluble polymers—acrylic and methacrylic acids, acrylamide and its derivatives, vinylpyrrolidone, etc. [5,6]. At the same time, the choice of an appropriate water-soluble photoinitiator is sometimes problematic for such compositions, since the most widely used water-soluble organic photoinitiators (camphoroquinone, thioxanthone derivatives, titanocenes, dyes, etc.) either absorb only small fraction of the visible light [1–3,5,6] or are photochemically unstable.

It has recently been shown that nanometer particles (NPs) of inorganic semiconductors, such as CdS, ZnO, TiO_2, Fe_2O_3, etc., could be successfully applied along with traditional organic photopolymerization initiators. Semiconductor NPs manifest quite high efficiency for the initiating of the photopolymerization of various monomers [7–14], they are stable and some of them, for example cadmium sulfide and iron(III) oxide, are sensitive to the visible light. Wide-band gap semiconductor NPs, such as ZnO and TiO_2, which have the absorption threshold in the ultraviolet part of the spectrum, can also be used as visible light-driven photoinitiators provided a dye-sensitizer is added to the photopolymerization composition [12,14,15]. Along with this, the most part of the reported examples of the semiconductor NPs-induced photopolymerization are focused on a narrow monomers range, mainly styrene, methylmethacrylate and some

* Corresponding author. Tel.: +380 44 525 0270/6662; fax: +380 44 525 6662.
E-mail addresses: alstroyuk@ukr.net, stroyuk@inphyschem-nas.kiev.ua (A.L. Stroyuk).

1010-6030/$ – see front matter © 2007 Elsevier B.V. All rights reserved.
doi:10.1016/j.jphotochem.2007.05.010

of its homologues [7,8,10–16]. The photopolymerization of water-soluble monomers in the presence of semiconductor NPs remains yet to be studied.

In the present work the photopolymerization of acrylamide (AA) in aqueous colloidal solutions of iron(III) oxide is investigated with the stress on primary photoinitiation processes. The results presented show that Fe_2O_3 NPs can be successfully used as inexpensive, efficient and visible light-sensitive photoinitiator of AA polymerization both in degassed and air-containing aqueous solutions.

2. Materials and methods

Reagent grade quality $FeCl_3$, acrylamide, $KBrO_3$, KBr, KI, all purchased from Aldrich, were used in the experiments. Colloidal iron(III) oxide solutions (1.5×10^{-3} M) were prepared via the prolonged (1–2 h) heating of 3×10^{-3} M $FeCl_3$ solution at 96–98 °C. Colloidal solutions were kept in the dark at 18–20 °C.

The irradiation of solutions (2.0 mL) was performed in quartz 1.0 cm parallel-sided optical cuvettes using the 1000 W high pressure mercury lamp in the narrow spectral domain with $\lambda = 310$–390 nm or with a 500 W incandescent lamp in the range of $\lambda > 400$ nm. In some experiments solutions were degassed before the irradiation. Light intensity was varied from 0.16×10^{-7} to 1.67×10^{-7} Einstein/s using the calibrated metal grids.

The AA concentration was determined by a photometric method based on the monomer bromination followed by the iodometric detemination of residual bromine. In typical procedure, 0.2 mL of an irradiated solution were added to the 8.0 mL of a mixture of 0.50 M H_2SO_4 and 0.11 M KBr. To this solution 0.8 mL of 0.05 M $KBrO_3$ were added. Resulting mixture was kept for 10–15 min in the dark at room temperature to achieve complete AA bromination. Then 1.0 mL of 2 M KI solution were added. In 5 min 0.1 mL aliquote was taken and mixed with 9.9 mL of 2.0 M potassium iodide solution. The monomer concentration was then calculated from the optical density of the resulting solution at 351 nm.

Initial photopolymerization rate R_p was determined as an average rate of the AA concentration decrease during the first 10–15 min of the photopolymerization (at the linear section of a kinetic curve). Quantum yield of the photopolymerization was calculated as $\Phi = R_p v_{cuv}/(1000I)$, where v_{cuv} is a solution volume (2 mL) and I is the absorbed light intensity. Molecular mass of polyacrylamide was determined using the single-point viscosimetry [17].

Absorption spectra were recorded on Specord 210 spectrophotometer. The XRD spectra were registered on DRON-3M diffractometer with the copper Kα line irradiation ($\lambda = 0.1541$ nm). TEM images were obtained using PEM-125K apparatus with accelerating voltage of 100 kV.

3. Results and discussion

3.1. Structural and optical properties of Fe_2O_3 NPs

Boiling of the aqueous iron(III) chloride solutions results in the salt hydrolysis and formation of brownish-red stable iron oxide colloids. An electrons diffraction (ED) pattern of freshly prepared colloidal Fe_2O_3 particles (Fig. 1a) consists of only two weak circles and a central halo indicating the most part of iron oxide particles be amorphous. The ageing of the colloidal solutions is accompanied by continuous crystallization of Fe_2O_3 particles as evident from an increase in the number of the circles in the ED pattern and their narrowing. The ED pattern of the Fe_2O_3 particles after 20 days ageing consists of at least 7 distinct reflexes (Fig. 1b) corresponding to the interplanar distances 1.54, 1.88, 2.16, 2.52, 3.04, 3.61 and 4.18 Å of hematite (α-Fe_2O_3) [18–21].

TEM image of the iron oxide particles aged for 20 days is presented on Fig. 1c. There are evidently two major fractions of the NPs on the TEM image: “small” 4–6 nm particles and “big”

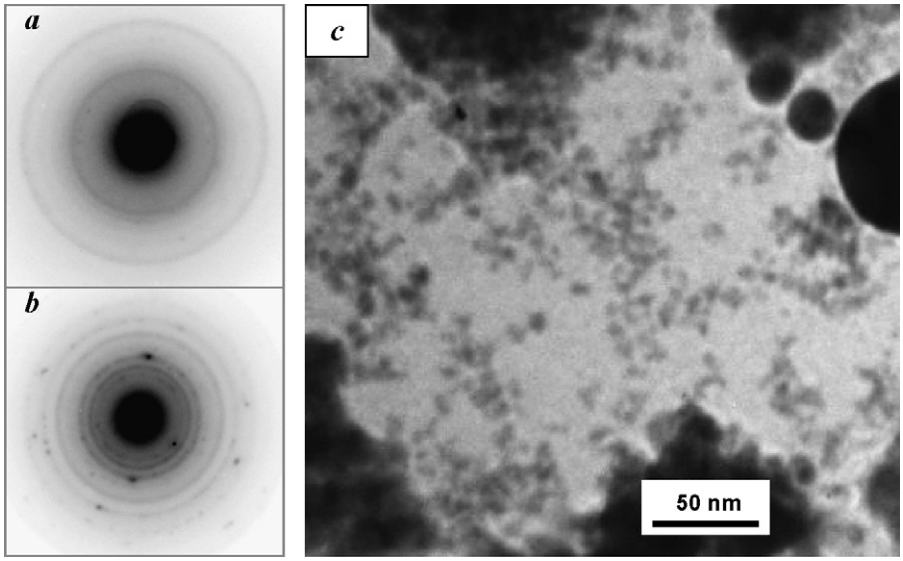

Fig. 1. Electron diffraction patterns (negative images) of freshly prepared (a) and aged for 20 days (b) colloidal Fe_2O_3 solution. (c) TEM image of Fe_2O_3 nanoparticles aged for 20 days.

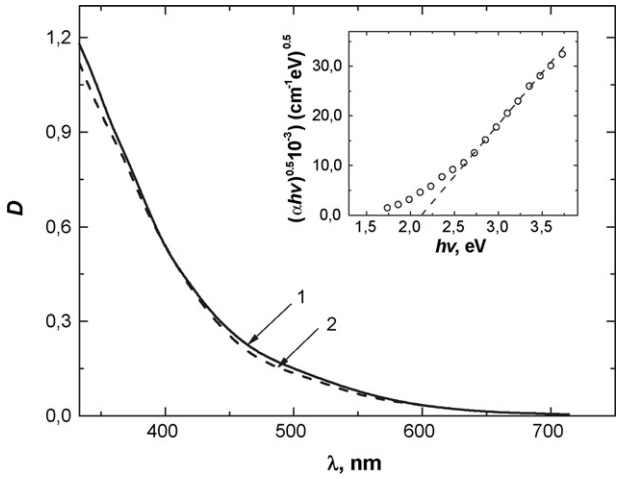

Fig. 2. Absorption spectra of freshly prepared (1) and aged for 20 days and (2) Fe_2O_3 colloids. $[Fe_2O_3] = 5 \times 10^{-4}$ M, optical path $l = 1.0$ cm. Inset: spectrum (2) in the coordinates $(\alpha h\nu)^{0.5}$–$h\nu$.

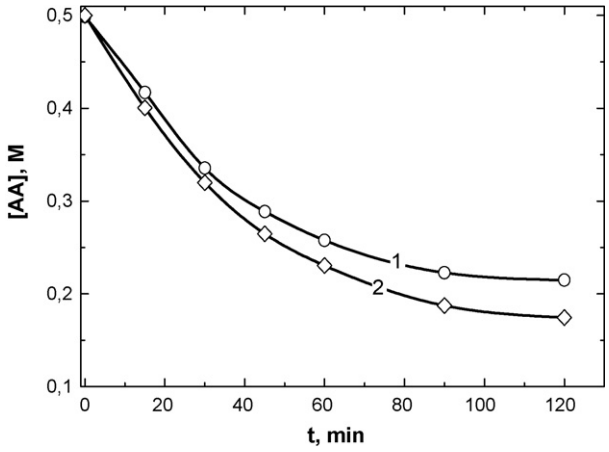

Fig. 3. Kinetic curves of the acrylamide polymerization in the presence of Fe_2O_3 NPs in air-exposed (1) and evacuated (2) solutions. $[Fe_2O_3] = 3 \times 10^{-4}$ M (aged for 20 days), $[AA]_0 = 0.5$ M, $I_0 = 1.67 \times 10^{-7}$ Einstein/s.

NPs, larger than 20–30 nm. Despite of the differences in the crystallinity, the absorption spectra of both freshly prepared and aged colloidal Fe_2O_3 solutions are almost identical and consist of featureless absorption band smoothly descending throughout the visible spectrum domain (Fig. 2). A section of the spectral curves with $h\nu > 2.5$ eV was found to be linear in the coordinates $(\alpha h\nu)^{0.5}$–$h\nu$, where $\alpha(h\nu) = 2303\rho D(h\nu)CM^{-1}l^{-1}$ (ρ is the density of hematite, 5.24 g/cm^3 [22], $D(h\nu)$ the optical density of the solution, corresponding to the quantum energy $h\nu$, C the colloidal solution concentration in g/cm^3, M the molar mass of iron(III) oxide and l is the optical path). It can be therefore concluded that the observed absorption band originates from an indirect interband electron transition in hematite NPs [23,24]. Extrapolation of the linear spectrum anamorphosis to the zero ordinate (see inset to Fig. 2) gives the band gap of Fe_2O_3 particles $E_g = 2.12 \pm 0.02$, the value being in accordance with the well-known E_g of the bulk hematite (2.0–2.2 eV [24–27]). Light absorbance at $h\nu < E_g$ is supposed to originate from defect states laying in the band gap near to the conduction (valence) band edge [23,24].

3.2. Kinetics of the acrylamide photopolymerization

Irradiation of the solutions, where AA and Fe_2O_3 NPs are both present, with the UV ($\lambda = 310$–390 nm) or visible light ($\lambda = 400$–600 nm) results in a gradual decrease of the monomer concentration and growth of the solution viscosity indicating a polymer formation (Fig. 3). In the absence of the iron oxide NPs, AA concentration remains constant at prolonged irradiation (3–4 h). It can be concluded that Fe_2O_3 NPs act as the photoinitiator of AA polymerization. There holds a balance between the mass of the monomer consumed to the moment when the photoreaction is stopped and the mass of a polymeric product, the fact indicating the photopolymerization be the sole path of monomer consumption.

Light absorption by Fe_2O_3 NP results in generation of the conduction band electrons (e^-_{CB}) and the valence band holes (h^+_{VB}). Primary radicals can, in principle, be produced in the monomer reactions with both e^-_{CB} and h^+_{VB}. If the photoinitiation of AA polymerization involves conduction band electrons, a fall of the photopolymerization rate after the admission of air into the reaction mixture can be expected, since the oxygen is an efficient electron acceptor. It was found though, that the photopolymerization rate decreases only slightly (~15%), when oxygen molecules are present in the solution (curves 1 and 2, Fig. 3). So, one can conclude that e^-_{CB} does not reduce neither oxygen nor the monomer, the valence band holes being apparently the sole participant of primary radicals generation.

The same conclusion can be derived from the evaluation of the energetic characteristics of the photopolymerization system components. The valence band potential (E_{VB}) of hematite is as positive as +1.85 V versus normal hydrogen electrode (NHE) at pH 14 [28]. The most part of the presented experiments were performed in neutral solutions with the initial monomer concentration $[AA]_0 = 0.5$ M. At pH 7 E_{VB}(α-Fe_2O_3) = +2.26 V (NHE). So, the conduction band potential of the colloidal iron(III) oxide NPs with $E_g = 2.12$ eV is also positive, $E_{CB} = +0.14$ V (NHE). This potential is apparently too low for one-electron reduction of oxygen ($E^0 = -0.33$ V, NHE [28]). Though an exact value of the AA reduction potential is not to be found in literature, it is known that the reduction potentials of acrylic acid derivatives are in general close to −1 V (NHE) [8,29]. Hence, the direct AA reduction by the Fe_2O_3 NPs conduction band electrons is also unfavorable.

The indirect monomer radicals generation via the AA reduction by the hydrogen atoms, which can form at the water reduction by e^-_{CB}, should also be regarded as improbable, since at pH 7 $E(H^+/H^\bullet) = -0.41$ V (NHE). Additional experiments showed that no molecular hydrogen forms even in trace amounts at prolonged irradiation of iron(III) oxide colloids. Summarizing, one can conclude that the most probable way of the primary radicals generation in the system under investigation is the AA oxidation by the Fe_2O_3 valence band holes.

It was found that the molecular mass of polyacrylamide (PAA) produced in air-containing solutions (0.7 ± 0.1)

Table 1
The quantum yields (Φ) and the initiation quantum yields (β) of the Fe_2O_3 NPs-initiated AA photopolymerization

No.	$[Fe_2O_3]$ $\times 10^4$, M	$[AA]_0$, M	$I_0 \times 10^7$, Einstein/s	Deaeration	Ageing, days	Φ	β
1	3.0	0.5	1.67	–	1	0.7	0.01
					4	5.6	0.7
					11	15.1	4.7
					20	17.6	5.5
2		0.2		+		3.3	3.6
		0.5				16.9	5.9
		0.9				41.0	6.0
3	0.6	0.5				37.0	8.7
	0.6					4.0	0.1
	2.0			–		17.6	5.0
	5.5					12.9	4.4
4	3.0		0.17	+	11	88.2	16.3
			0.33			61.5	15.4
			0.55			47.1	15.0
			0.83			33.0	11.1

$\times 10^6$ g/mole, is substantially lower than that of the polymer obtained from degassed solutions $(1.2 \pm 0.1) \times 10^6$ g/mole. This can be due to the participation of oxygen in the chain termination reactions [30,31].

In the following section basic factors affecting the rate of AA polymerization (summarized in Table 1), that is the aging duration and NPs concentration, initial monomer concentration and the light intensity, are discussed.

3.3. The age and concentration of Fe_2O_3 nanoparticles

It was found that the photocatalytic activity of Fe_2O_3 NPs in the photoinitiation of AA polymerization depends notably upon the duration of the colloidal solution ageing (Table 1, series 1).

Fig. 4 demonstrates that freshly prepared Fe_2O_3 NPs are inert in the photoreaction. Upon the ageing of Fe_2O_3 NPs during 1–10 days a constant growth of the rate of AA photopolymerization is observed, the stationary photoactivity being achieved after 12–20 days.

Taking into consideration above-discussed TEM results, the growth of the photocatalytic activity of Fe_2O_3 NPs upon ageing can be associated with gradual crystallization of the colloidal semiconductor and a decrease of the fraction of amorphous iron(III) oxide. It is well-known that oxide semiconductors, for example, TiO_2, manifest noticeable photocatalytic activity only when being in the crystalline state [32–34]. Very fast recombination processes in amorphous semiconductors [35] result evidently in the suppression of the photochemical reactions.

Photocatalytic AA polymerization in the presence of air is of considerable interest first of all from the practical viewpoints, for example, for the photochemical PAA synthesis or for the design of photocurable compositions [31,36]. So, the kinetics of the

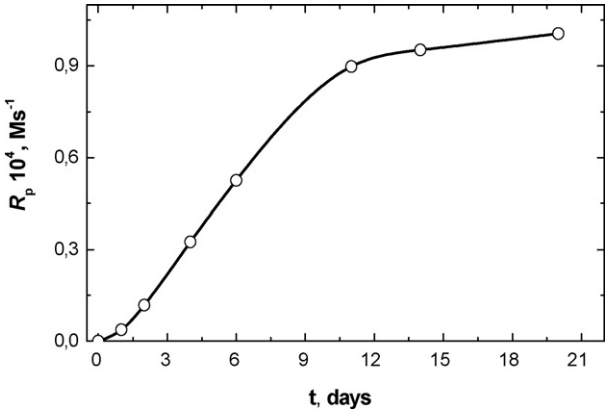

Fig. 4. Dependence between the ageing duration of colloidal Fe_2O_3 solution and the rate of acrylamide photopolymerization in the presence of air. $[Fe_2O_3] = 3 \times 10^{-4}$ M, $[AA]_0 = 0.5$ M, $I_0 = 1.67 \times 10^{-7}$ Einstein/s.

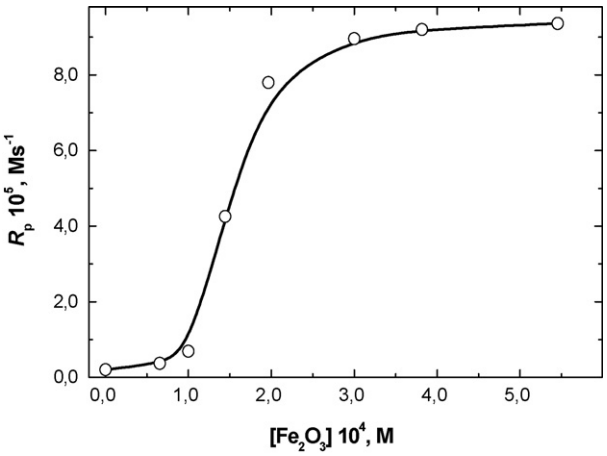

Fig. 5. The rate of acrylamide photopolymerization in the presence of air vs. the molar Fe_2O_3 concentration. $[AA]_0 = 0.5$ M, $I_0 = 1.67 \times 10^{-7}$ Einstein/s.

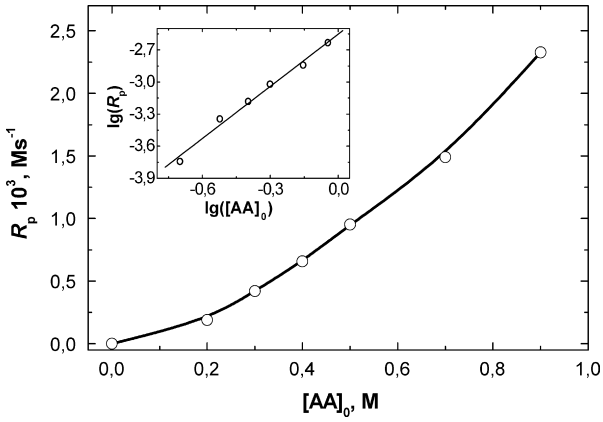

Fig. 6. The rate of AA photopolymerization in deaerated solution vs. the initial monomer concentration $[AA]_0$. $[Fe_2O_3] = 3 \times 10^{-4}$ M (aged for 20 days), $I_0 = 1.67 \times 10^{-7}$ Einstein/s. Inset: R_p–$[AA]_0$ dependence in logarithmic coordinates.

photocatalytic polymerization was studied mostly in air-exposed systems.

Fig. 5 and Table 1 (series no. 3) describe the dependence of the photopolymerization rate upon the molar Fe_2O_3 concentration. It has S-like shape (Fig. 5) originating probably from the efficient inhibition by oxygen at low photocatalyst content. When the Fe_2O_3 concentration grows, light absorbance of the photopolymerization system and the primary radicals concentration grow too, making the inhibitive oxygen effect less pronounced. It was found, indeed, that at low photoinitiator concentrations ($[Fe_2O_3] = 0.6 \times 10^{-4}$ M; Table 1, series 3) evacuation of the reaction mixtures results in an almost 10-fold R_p increase.

At $[Fe_2O_3] > 3 \times 10^{-4}$ M saturation of the light absorption is achieved and further growth of the iron oxide concentration does not affect considerably the photopolymerization rate. When complete light absorbance is achieved, the photopolymerization rate remains virtually constant in a wide range of the nanoparticles concentration (Fig. 5). One can therefore conclude that semiconductor NPs do not participate in the termination of growing polymer chains. This conclusion is supported also by the fact that the PAA molecular mass do not noticeably change at the variation in the iron oxide concentration from 3×10^{-4} to 1.5×10^{-3} M.

At the precipitation of PAA by acetone semiconductor NPs are occluded by the polymer and precipitated as well. However, treatment of the PAA with small portions of diluted sulfuric acid results in visible dissolution of Fe_2O_3 NPs. So, in contrast to many traditional organic photoinitiators, iron oxide NPs can be easily removed from the final product, which allows to synthesize pure PAA by the photochemical reaction. Along with that, iron oxide NPs have two more advantages over the majority of the traditional organic photoinitiators: they are sensitive to a wide visible light domain and function efficiently in air-exposed solutions.

3.4. Initial monomer concentration

The photopolymerization rate grows non-linearly at the increase in the initial AA concentration (Fig. 6 and Table 1, series 2). Curve in Fig. 6 is linear in logarithmic coordinates (see inset to Fig. 6), the kinetic reaction order by the monomer concentration being $n_{AA} = 1.5$ (±0.1).

For free-radical polymerization of vinyl monomers induced by the photochemical destruction of traditional organic photoinitiators, linear dependence between the photopolymerization rate and the initial monomer concentration is usually observed, i.e. $n_{AA} = 1.0$ [4,37,38]. Deviation of n_{AA} from the unity can be associated with the AA participation in the primary radicals generation [4,37,38], which will be discussed further.

3.5. The light intensity

Dependence between the R_p and light intensity I_0 in the case of air-exposed solutions (Fig. 7, curve 1; Table 1, series 4) is also S-shaped, similarly to the dependence of the photopolymerization rate upon the Fe_2O_3 concentration. At the same time, the R_p–I_0 dependence obtained in degassed solutions (Fig. 7, curve 2) is quite typical for the free-radical photopolymerization [4,37,38].

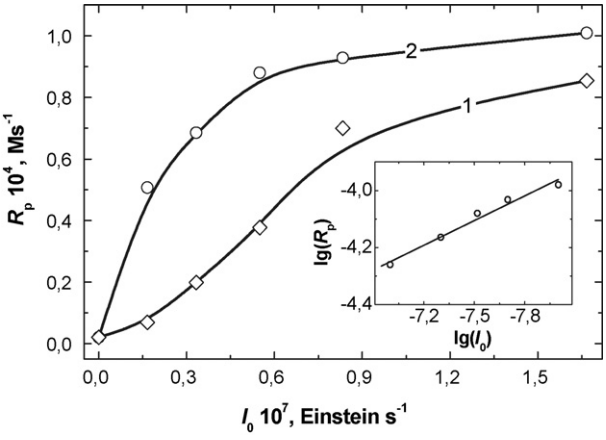

Fig. 7. The rate of acrylamide photopolymerization in the presence of air (1) and deaerated (2) solution vs. the light intensity I_0. $[Fe_2O_3] = 3 \times 10^{-4}$ M (aged for 20 days), $[AA]_0 = 0.5$ M. Inset: Dependence (1) in logarithmic coordinates.

Kinetic order of the photoreaction by the light intensity, determined from the logarithmic linearization of the curve 2 from Fig. 7 (see inset to Fig. 7) was found to be $n_I = 0.38$ (± 0.07). The value is close to 0.5, which is known to hold for free-radical polymerization with photochemical initiation and recombinative chain termination [4,36]. Some negative deviation of n_I from the expected value is probably associated with the phenomenon, general for the photochemistry of semiconductor NPs – growth of the efficiency of the recombination processes at an increase in the light intensity (see for example refs. [32,39–42]). This phenomenon is apparently responsible for the lowering of the photopolymerization quantum yield Φ from 88.2 to 16.9 at the increase in the light intensity from 0.17×10^{-7} to 1.67×10^{-7} Einstein/s (Table 1, series nos. 2–4). The light intensities optimal for the photocatalytic AA polymerization in air-exposed solutions were found to be $0.6–0.9 \times 10^{-7}$ Einstein/s (Fig. 7, curve 1).

3.6. Mechanism of AA photopolymerization

Considering all above-discussed experimental results, the following photopolymerization mechanism can be proposed:

$$Fe_2O_3 + h\nu \rightarrow (e^-_{CB} + h^+_{VB})Fe_2O_3 \quad (1)$$

$$e^-_{CB} + h^+_{VB} \rightarrow \Delta H \quad (2)$$

$$e^-_{CB} + Fe^{III}_2O_3 \rightarrow Fe^{II}Fe^{III}O_3 \quad (3)$$

$$h^+_{VB} + AA \underset{-H^+}{\longrightarrow} AA^\bullet \quad (\beta) \quad (4)$$

$$AA^\bullet + AA \rightarrow AA_2^\bullet + AA \rightarrow \cdots \rightarrow AA_n^\bullet \quad (k_p) \quad (5)$$

$$AA_n^\bullet + AA_n^\bullet \rightarrow AA_{2n} \quad (k_t) \quad (6)$$

In the above scheme the process (1) corresponds to the photogeneration of the non-stationary charge carriers. Step (2) summarizes all the non-radiative energy dissipation processes with the heat ΔH release. Conduction band electrons can be consumed, along with the process (2), via the lattice iron(III) reduction (reaction (3)). The primary radicals generation occurs at the monomer oxidation by the valence band holes (reaction (4)). Oxidation of the monomer by the photogenerated valence band holes is expected to give a cation-radical $A^{\bullet+}$. At the same time, the acrylamide photopolymerization is of free-radical nature. One can therefore suppose that the monomer cation-radical transforms into the free-radical $A^\bullet$, one of the possible ways for this transformation be proton removal from $A^{\bullet+}$.

It should be noted that low sensitivity of the systems under investigation toward the oxygen can originate from a particular nature of the photoinitiation process. In classical photopolymerization one or a pair of active primary radicals are generated at the photoinduced decomposition of a photoinitiator. The fast consumption of these radicals in reactions with oxygen is the reason under the inhibiting effect of air and the appearance of induction periods. In our case, the primary radicals form directly at the monomer oxidation (4). Oxygen is known to be capable to bind into the growing macroradical without substantial suppression of the polymerization [37,38]. So, the elimination of the step of the formation of active primary radicals from a photoinitiator could be responsible for the low sensitivity of our systems towards the presence of oxygen.

The rate of the photoinitiation (R_{in}), chain propagation (R_p) and chain termination (R_t) steps can be described by the following expressions:

$$R_{in} = \beta[AA]I \quad (7)$$

$$R_p = k_p[AA^\bullet][AA] \quad (8)$$

$$R_t = k_t[AA^\bullet]^2 \quad (9)$$

Taking into account that the photoinitiation rate at an initial stage of the photopolymerization is equal to the termination rate and assuming that the chain growth rate does not change with the chain length [37,38], one can derive the expression for the stationary concentration of radicals:

$$[AA^\bullet] = \left(\frac{\beta}{k_t}\right)^{0.5} [AA]^{0.5} I^{0.5} \quad (10)$$

Combining (8) and (10) we obtain the following kinetic expression

$$R_p = \left(\frac{k_p}{k_t^{0.5}}\right) \beta^{0.5} [AA]^{1.5} I^{0.5} \quad (11)$$

The exponents at the monomer concentration and the light intensity in (11) agree well with those obtained experimentally, supporting the proposed mechanism of the photocatalytic AA polymerization.

3.7. Quantum yields of the photoinitiation

Quantum yields of the photoinitiation of the AA polymerization (β) can be determined from the expression (11) using the constants ratio $k_p/k_t^{1/2}$ tabulated for various monomers ($k_p/k_t^{1/2} = 4.7$ at 20 °C for AA [37]). It can be seen from Table 1 that the photoinitiation quantum yield in general does not exceed 10^{-2}. Low quantum efficiency of the primary radicals generation could possibly originate from the very fast non-radiative electronic energy degradation in Fe_2O_3 NPs [43]. According to [35,43], fast non-radiative relaxation of the excitation energy in the iron oxide NPs (characteristic times of the photogenerated charge carriers decay are below 60–70 ps regardless of the oxide modification) is due to high density of states in the allowed bands and surface defect states.

4. Conclusions

Photocatalytic activity of the hematite nanoparticles in the photoinitiation of the acrylamide polymerization in aqueous solutions has been found, quantum yields of the photoinitiation being lower than 10^{-2}.

It has been found that Fe_2O_3 NPs-initiated acrylamide photopolymerization proceeds with comparable effectiveness both in deaerated and in air-exposed aqueous solutions at comparatively low photoinitiator concentrations ($[Fe_2O_3] < 1 \times 10^{-3}$ M) under the UV (310–390 nm) and visible light (400–600 nm)

and yields polyacrylamide with relatively high molecular mass (1.2×10^6 g/mole in degassed solutions and 0.7×10^6 g/mole in the air-containing systems). The semiconductor can be easily removed from the polymeric product by acidic treatment.

Kinetics of the photocatalytic polymerization has been studied and the optimal reaction conditions determined. A scheme of the photopolymerization mechanism has been proposed. The photoinitiation stage is supposed to proceed with the participation of acrylamide radicals generated via the monomer oxidation by the photogenerated iron oxide valence band holes.

References

[1] A.B. Scranton, C.N. Bowman, R.W. Peiffer (Eds.), Photopolymerization: Fundamentals and Applications, ACS, New York, 1997.
[2] D. Belfield (Ed.), Photoinitiated Polymerization, C.H.I.P.S, 2003.
[3] A.I. Kryukov, V.P. Sherstyuk, I.I. Dilung, Electron Phototransfer and its Application, Naukova dumka, Kyiv, 1982.
[4] V.A. Kargin (Ed.), Encyclopedia of Polymers, Sovetskaya Enziklopedia, Moscow, 1977.
[5] R. Liska, F. Schwager, C. Maier, R. Cano-Vives, J. Stampfl, J. Appl. Polym. Sci. 97 (2005) 2286.
[6] N. Davidenko, O. Garcia, R. Satsre, J. Biomater. Sci. Polym. Ed. 14 (2003) 733.
[7] A.J. Hoffmann, G. Mills, H. Yee, M.R. Hoffmann, J. Phys. Chem. 96 (1992) 5546.
[8] A.J. Hoffmann, H. Yee, G. Mills, M.R. Hoffmann, J. Phys. Chem. 96 (1992) 5540.
[9] C. Damm, J. Photochem. Photobiol. A: Chem. 181 (2006) 297.
[10] C. Dong, X. Ni, J. Macromol. Sci. A41 (2004) 547.
[11] A.L. Stroyuk, V.M. Granchak, S.Ya. Kuchmiy, Theor. Exp. Chem. 37 (2001) 170.
[12] A.L. Stroyuk, V.M. Granchak, A.V. Korzhak, S.Ya. Kuchmiy, J. Photochem. Photobiol. A: Chem. 162 (2004) 339.
[13] A.L. Stroyuk, V.M. Granchak, S.Ya. Kuchmiy, Theor. Exp. Chem. 37 (2001) 347.
[14] R. Ojah, S.K. Dolui, J. Photochem. Photobiol. A: Chem. 172 (2005) 121.
[15] A.L. Stroyuk, V.M. Granchak, S.Ya. Kuchmiy, Theor. Exp. Chem. 38 (2002) 324.
[16] R. Ojah, S.K. Dolui, Solar Energy Mater Solar Cells 90 (2006) 1615.
[17] M.H.R. Fanood, M.H. George, Polymer 28 (1987) 2244.
[18] P. Deb, T. Biswas, D. Sen, A. Basumallick, S. Mazumder, J. Nanoparticle Res. 4 (2002) 91.
[19] C. Garcia, Y. Zhang, F. DiSalvo, U. Wiesner, Angew. Chem. Int. Ed. 42 (2003) 1526.
[20] L. Casas, A. Roig, E. Molins, J.M. Greneche, J. Asenjo, J. Tejada, Appl. Phys. A 74 (2002) 591.
[21] K. Woo, H.J. Lee, J.-P. Ahn, Y.S. Park, Adv. Mater. 15 (2003) 1761.
[22] I.T. Goronovski, Yu.P. Nazarenko, E.F. Nekryatch, Handbook of Chemistry, Naukova Dumka, Kyiv, 1974.
[23] V.I. Fistul, Introduction into the Semiconductor Physics, Vysshaya Shkola, Moscow, 1984.
[24] N.B. Hannay (Ed.), Semiconductors, Chapman & Hall, London, 1962.
[25] W. Feng, D. Nansheng, Chemosphere 41 (2000) 1137.
[26] U. Bjorksten, J. Moser, M. Grätzel, Chem. Mater. 6 (1994) 858.
[27] M. Gori, H.-R. Grüniger, G. Calzaferri, J. Appl. Electrochem. 10 (1980) 345.
[28] B.C. Faust, M.R. Hoffmann, D.W. Bahnemann, J. Phys. Chem. 93 (1989) 6371.
[29] M.M. Baizer, H. Lund (Eds.), Organic Electrochemistry, Marcel Dekker, N.Y. & Basel, 1988.
[30] M.H. George, A. Ghosh, J. Polym. Sci. Polym. Chem. Ed. 16 (1978) 981.
[31] M. Biernat, G. Rokicki, Polimery (polish Ed.) 50 (2005) 631.
[32] M. Grätzel (Ed.), Energy Resources through Photochemistry and Catalysis, Academic Press, N.Y, 1983.
[33] A. Fujishima, T.N. Rao, D.A. Tryk, J. Photochem. Photobiol. C: Rev. 1 (2000) 1.
[34] U. Diebold, Surf. Sci. Rep. 48 (2003) 53.
[35] J.Z. Zhang, J. Phys. Chem. B 104 (2000) 7239.
[36] M. Awokola, W. Lenhard, H. Löffler, C. Flosbach, P. Frese, Prog. Polym. Coat. 44 (2002) 211.
[37] H.S. Bagdasaryan, Theory of Radical Polymerization, Nauka, Moscow, 1966.
[38] C.H. Bamford, W.G. Barb, A.D. Jenkins, P.F. Onyon (Eds.), The Kinetics of Vinyl Polymerization by Radical Mechanisms, Butterworths Scientific Publications, London, 1958.
[39] S.V. Gaponenko, Optical Properties of Semiconductor Nanocrystals, University Press, Cambridge, 1996.
[40] Y. Nosaka, M.A. Fox, J. Phys. Chem. 90 (1986) 6521.
[41] A. Yu, Gruzdkov, E.N. Savinov, V.N. Parmon, Chem. Phys. (Russ. Ed.) 7 (1988) 44.
[42] D. Duonghong, J. Ramsden, M. Grätzel, J. Am. Chem. Soc. 104 (1982) 2977.
[43] V.A. Nadtochenko, N.N. Denisov, V.Yu. Gak, S.E. Gostev, A.A. Titov, O.M. Sarkisov, V.V. Nikandrov, Izvestia AN: Ser. Khim. (Russ. Ed.) 3 (2002) 426.